2019 IEEE World Haptics Conference (WHC)
Tokyo, Japan
9-12 July 2019

Tasbi: Multisensory Squeeze and Vibrotactile Wrist Haptics for Augmented and Virtual Reality

Evan Pezent[†‡], Ali Israr[†], Majed Samad[†], Shea Robinson[†],
Priyanshu Agarwal[†], Hrvoje Benko[†], and Nick Colonnese[†]

***Abstract*— Augmented and virtual reality are poised to deliver the next generation of computing interfaces. To fully immerse users, it will become increasingly important to couple visual information with tactile feedback for interactions with the virtual world. Small wearable devices which approximate or substitute for sensations in the hands offer an attractive path forward. In this work, we present Tasbi, a multisensory haptic wristband capable of delivering squeeze and vibrotactile feedback. The device features a novel mechanism for generating evenly distributed and purely normal squeeze forces around the wrist. Our approach ensures that Tasbi's six radially spaced vibrotactors maintain position and exhibit consistent skin coupling. In addition to experimental device characterization, we present early explorations into Tasbi's utility as a sensory substitution device for hand interactions, employing squeeze, vibration, and pseudo-haptic effects to render a highly believable virtual button.**

I. Introduction and Background

Advances in motion tracking, optics, displays, and computer graphics have revolutionized head mounted displays (HMD) for augmented reality (AR) and virtual reality (VR). With increasing research and development into AR/VR, these devices are positioned to reinvent computer interfaces in ways similar to the cellphones and personal computers that preceded them. The addition of haptic feedback to AR/VR is appealing, since touch feedback can close the action-confirmation loop, reduce cognitive load, and increase performance [1]. However, most widely used AR/VR interfaces today leave much to be desired in terms of haptic feedback as they offer little more than simple vibration at best. While more advanced grasping, fingertip, and glove type devices [2], [3] show promise, they currently face a number of challenges regarding encumbrance, locating actuators, grounding forces, and power requirements. Because of these unresolved complexities, more practical and imminent devices are desired to render feedback in AR/VR.

Wristband or bracelet type devices are an attractive location for AR/VR interfaces and offer several advantages. First, wristbands allow for a reasonable design space in terms of acceptable weight, size, and power needs. Secondly, wrist bands leave the hands free, which is important for AR as they allow the hands to manipulate the physical world unhindered. Finally, wrist bands are socially acceptable and even fashionable. A variety of feedback modalities have been explored for wrist and arm haptics, with two of the most common being vibrotactile feedback and squeeze feedback.

[†]Facebook Reality Labs, Redmond, WA 98052, USA. [‡]Mechatronics and Haptic Interfaces Laboratory, Dept. of Mechanical Engineering, Rice University, Houston, TX 77005, USA.

Fig. 1. Tasbi is a multisensory haptic wristband capable of delivering squeeze and vibrotactile feedback for a variety of uses in AR/VR.

A. Vibrotactile Feedback

Several researchers have investigated placing vibrotactors (or tactors) on the wrist and arm. Chen et al. [4] compared placing planar arrays of tactors on the dorsal versus the volar side of the wrist. Matscheko et al. [5] further studied arranging tactors dorsally versus radially, concluding that placing tactors around the wrist circumference was best. Following their advice, Carcedo et al. [6] developed a wristband with radially spaced tactors. They tested variations of a band with 3, 4, 5, and 6 equally spaced tactors, and found that users can reliably detect five vibration motors around the wrist. However, their design did not attempt to isolate vibration transfer between adjacent motors. Hong et al. [7] addressed issues of vibration transfer by separating tactors with thin elastic thread. They concluded that in this configuration, up to eight tactors can increase accuracy in a guidance task. While results of tactor placement and discretization are varied, it is generally agreed that proper tactor contact with the skin is critical to achieving optimal vibration transfer.

B. Squeeze Feedback

Squeeze feedback is thought to be less attention demanding than vibration [8], provides more intimate feedback similar to how one human might get the attention of another [9], [10], and may elicit affective or emotional responses [11]. Most squeezing devices employ one or more motors to tension bands around the arm [10], [12]–[16], and are characterized by generating both inward and tangential forces (i.e. skin-stretch) on the skin. Other devices have used cams and linkages to create purely compressive forces [17]–[19]. Gupta et al. [20] addressed the size concerns of the aforementioned devices by employing shape-memory alloys.

978-1-5386-9461-9/19/$31.00 © 2019 IEEE

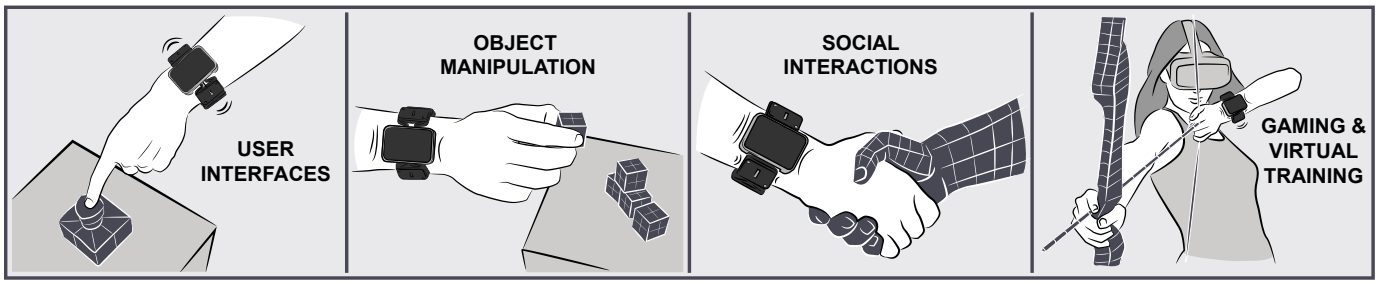

Fig. 2. Tasbi enables a variety of interactions with the virtual world. Vibrotactile feedback may substitute for fingertip contact with virtual buttons or other types of user interfaces, while squeeze may convey the weight or stiffness associated with manipulating virtual objects. Squeeze and vibration can further add to telepresence and remote social interactions such as hand shaking or holding, and can also provide immersive feedback for gaming and training.

However, this approach required high power and insulation to shield users from heat. Pohl et al. [21] used pneumatically actuated pockets to create uniform compression akin to a blood pressure cuff, but this low bandwidth approach could limit AR/VR interactions.

C. Multisensory Feedback

Most devices discussed so far were developed for notification type interactions, and thus can only offer limited experiences for AR/VR. One way in which wristband devices can be made more applicable to AR/VR is by enabling *multisensory* feedback. Combining squeeze and vibration could not only provide a richer cue set with higher information throughput, but also the ability to accurately depict everyday interactions, which are inherently mutlisensory, in AR/VR (Fig. 2).

Despite a high volume of research on vibration and squeeze feedback alone, a relatively limited number of devices have implemented both modalities into a multisensory wearable. Dunkelberger et al. developed the MISSIVE [22], which combines separate bands for vibration and squeeze to render language. Aggravi et al. presented a forearm device [23] that incorporated squeeze and four tactors into the same band, but did not address the fact their design causes tactors to translate on the skin, which likely confuses users.

D. Contribution

In this paper, we present **Tasbi** (**T**actile **A**nd **S**queeze **B**racelet **I**nterface), a multisensory haptic wristband for AR/VR (Fig. 1). We hypothesize that combining robust forms of squeeze and vibration feedback into a single device will enable a richer haptic experience (Fig. 2). Our design (Section II) introduces a novel squeezing mechanism which addresses issues with previous squeezing devices, namely size and the ability to generate entirely normal forces, while maintaining high force output and bandwidth. The device incorporates a six vibrotactor band which has been specially designed to eliminate undesired translation and vibration transfer. In Section III we characterize squeezing capabilities and provide estimates of force and bandwidth useful to future designers. Section IV presents initial explorations into using Tasbi for sensory substitution, and details a unique virtual button interaction which leverages squeeze, vibration, and control-display ratio based pseudo-haptics. Finally, in Section V we present our conclusions and future plans.

II. Device Design

We aimed to achieve a wrist-watch form factor of approximately $50\times50\times15$ mm in size with a total weight less than 200 grams, without sacrificing force output and bandwidth. Further, we decided the device should emit little audible noise to avoid annoying or confusing users. Finally we deemed it necessary to keep total power consumption below 2 W so as to not dissipate an uncomfortable amount of heat on users' skin.

A. Squeeze Mechanism

While a few novel approaches to squeeze actuation exist, most devices use a similar scheme where one or more rotational actuators are used to directly wind a band element into an actuator housing [10], [12]–[16]. While this approach is straightforward, it presents two main issues (Fig. 3-a). First, directly tensioning the band itself gives rise to an unequal distribution of forces where there are concentrated tangential shear forces on the sides of the arm, and smaller normal forces on the underside. Furthermore, this results in non-trivial squeeze force losses due to friction between the band and skin. Second, because this method causes the band to translate along the skin, it does not allow for embedding vibrotactile elements in the band since they would consequently translate too. Maintaining the radial positions of the vibrotactors is key since their movement would decrease user identification rates and possibly cause discomfort. Some devices have circumvented this issue by using two separate bands: one for generating squeeze, and one for housing vibrotactors [22]. However, this approach is less than ideal for a wrist-watch form factor and complicates donning and doffing the device.

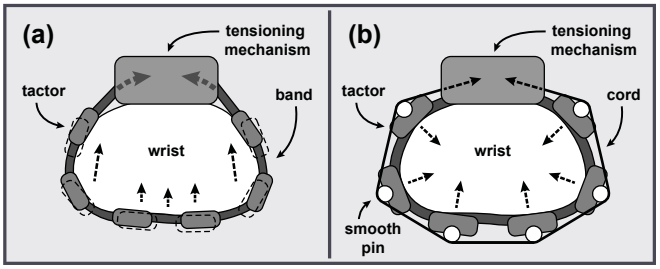

Fig. 3. **(a)** Typical constricting-band approaches to squeeze produce non-uniform and tangential forces which would cause embedded tactors to shift. **(b)** Our decoupled approach aims to produce pure, uniform normal forces.

Tasbi solves these problems by decoupling squeeze actuation from the wrist band and vibrotactors. This is accomplished by means of small diameter, flexible UHMWP cord, (trade name Dyneema/Sprectra) which wraps circumferentially around the exterior of the band (Fig 3-b). Tensioning this cord, not the band, creates squeeze forces. Friction is minimized by separating contact between the cord and band with smooth polished stainless steel pins placed directly above each vibrotactor. This mechanism results in cord tension being transmitted as an inward force approximately normal to the vibrotactor. Because friction between the pin and cord is small, little tangential force should be transmitted to the band, and as a result each vibrotactor should maintain its radial position around the circumference of the wrist. Eliminating friction and tangential forces also allows for a smaller actuator, since most power is ideally converted to purely normal squeeze force.

Early testing suggested that approximately 10 N of cord tension would be required to achieve an appropriate range of squeeze stimuli. Several tensioning mechanisms and actuators were initially considered. For ease of implementation and control, a electromechanical approach, as opposed to pneumatic or other exotic approaches, was decided. We used a 12 mm brushed DC motor coupled to a 100:1, 13 mm strain-wave gear unit from Harmonic Drive. These drives offered a set of characteristics we deemed necessary to fully realize Tasbi: (1) a sufficiently high torque reduction, (2) low audible noise due to having zero backlash, and most importantly (3) compactness superior to conventional gear units. The DC motor and Harmonic gear unit are contained within a 50×30×15 mm housing which rests on the dorsal side of the user's wrist. Attached to the output of the gear unit is a 10 mm diameter spool. Both ends of the cord terminate to the either side of the spool so that the take-up rate is doubled. The cord is redirected internally over additional smooth pins to exit at the center of the main housing.

B. Vibrotactile Band

The band contains six vibrotactor units. Each unit consists of a plastic housing in which the vibrotactor is press fit. The vibrotactors are 2.5 VAC, 10 mm linear resonant actuators (LRA) with resonance of 150 to 200 Hz. Directly above the vibrotactor is a groove for one of the aforementioned smooth pins. The distance from skin to the pin was optimized so that the UHMWP cord would clear and not rub against the user's skin. A lid secures each vibrotactor and pin in place.

Each tactor unit is clipped in between polyurethane rubber sidings via T-shaped joints. Tactor power cables are embedded within the rubber siding and enter the main housing through openings on both sides. The elasticity and geometry of the sidings allows the band to be stretched over the user's hand during the donning and doffing process and reduces vibration transfer between adjacent tactor units. Tasbi has an nominal inner circumference of approximately 150 mm, equal to the 50th percentile female wrist circumference. Thus for most users, the band provides a light amount of passive squeeze to ensure a comfortable initial fit.

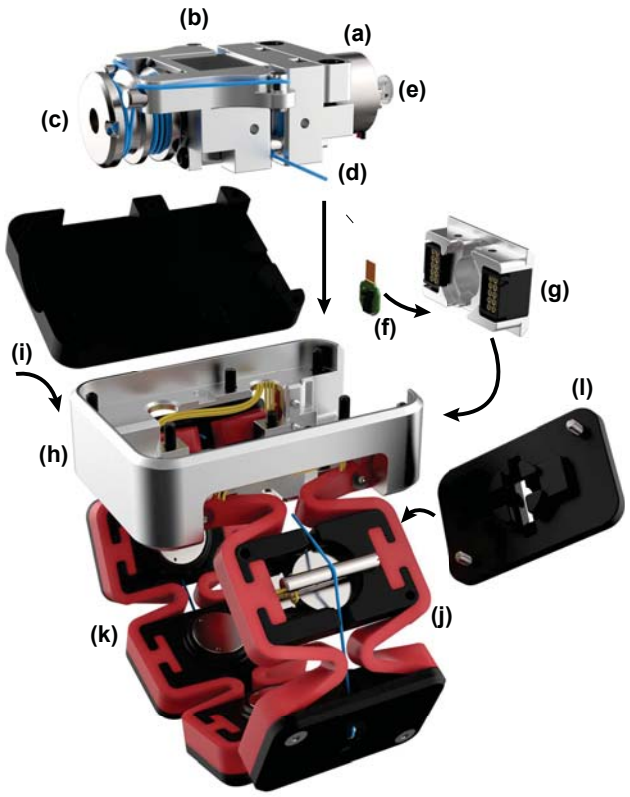

Fig. 4. Exploded view of Tasbi (color added for clarity). The squeeze mechanism consists of a 12 mm DC motor **(a)** and a 13 mm Harmonic Drive gearbox **(b)** which drives a two-sided spool **(c)** to create tension in a UHMWP cord **(d)**. Control feedback is provided through an optical encoder consisting of a reflective code wheel **(e)** and optoelectronic sensor **(f)**. The sensor is epoxied into the rear housing panel **(g)** which also contains two 10-pin connectors for all electronics. The drive assembly **(a-e)** drops into the main housing **(h)** and is secured in place with a housing lid **(i)**. Each vibrotactor unit **(j)** contains a 10 mm LRA vibrotactor and a smooth stainless steel pin to convert cord tension into normal force. Vibrotactor units are clipped into elastic sidings **(k)** and secured with lids **(l)**.

C. Feedback and Control

Closed-loop squeeze control is achieved via incremental encoder feedback placed on the motor side of the mechanism and an externally located servo controller operating in current control mode. The encoder and controller are interfaced through a host PC using a Quanser Q8-USB digital acquisition (DAQ) board and the C++ based Mechatronics Engine and Library. The motor position loop is closed in software with a proportional-derivative (PD) control law running at 1000 Hz. All six vibrotactors are controlled through a MOTU 24Ao sound card connected to the host PC over USB. We developed custom synthesizer software to generate ASR (Attack-Sustain-Release) amplitude envelopes with adjustable pitch, modulation, and waveform to deliver a wide range of vibration stimuli. Commands for squeeze and vibration can be sent to a server application over UDP or shared memory, enabling plug-and-play with VR content creation software such as Unity or Unreal Engine. The bracelet itself is connected to the external motor driver, DAQ, and sound card through two 10-pin connectors on its back panel.

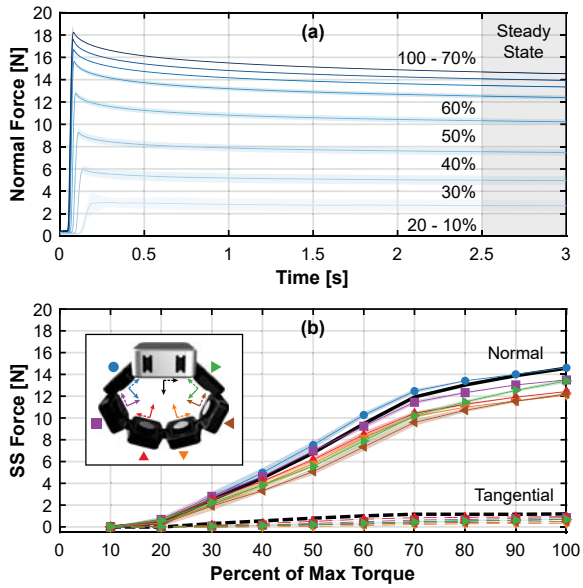

Fig. 5. **(a)** Representative responses for each torque step. **(b)** Steady state normal vs. tangential forces for each vibrotactor. All curves represent a mean, with standard deviation represented by shaded areas.

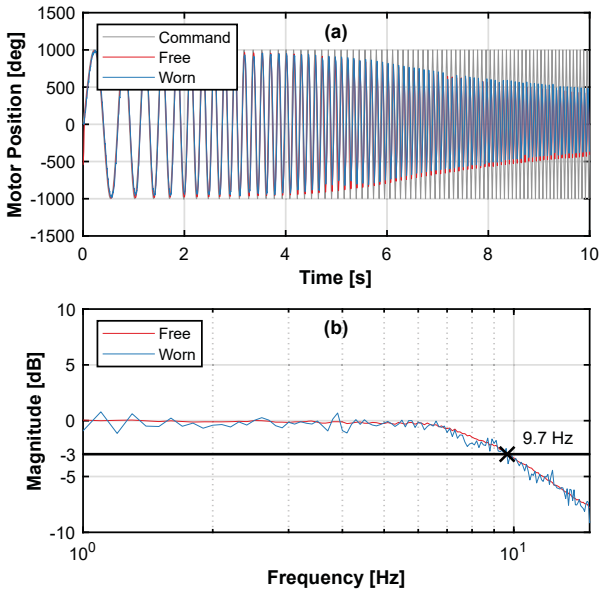

Fig. 6. **(a)** Motor position response to a 1-to-15 Hz chirp command for both free and user worn conditions. **(b)** Magnitude of the experimental transfer function. The closed-loop bandwidth is 9.7 Hz, defined by the -3 dB cutoff.

III. Squeeze Characterization

We next characterized Tasbi's squeezing capabilities. We created a fixture containing two ATI Nano17 F/T sensors; one remained fixed under the main housing for referencing, and the other was able to relocate under any tactor housing. The device was stretched over the fixture with the band center axis oriented upward so that gravity would not affect normal and tangential force measurements. The tensioning mechanism, initially with the cord loose, was commanded to step to a certain percentage of the max motor torque, hold for three seconds, and then return to the loose position. Force measurements were taken underneath the main and tactor housings in both the normal and tangential directions. This procedure was repeated ten times for each of ten torque levels from 10% to 100% of the maximum motor torque (3.21 mNm). The full test was repeated for each of the six tactor housings.

Fig. 5-a shows the force response under a representative tactor for each torque level. For torques above 50% there is a noticeable relaxing effect, most likely due to the material properties of the plastic housings and UHMWP tensioning cord. Torque levels below 20% produce little to no force output, revealing some dead band in the tensioning mechanism due to friction in the drive components. Fig. 5-b shows the "steady state" (i.e. the mean of the last half-second of the responses in Fig. 5-a) normal and tangential forces under each tactor. Importantly, we can see that there is negligible tangential force, with the force distribution being almost entirely normal and thus satisfying our design goals. The more proximal tactor housings have a higher normal force than the distal tactor housings, which is likely due to cord tension drop-off between adjacent tactors as a result of pin friction. There is also some bias, with left-side normal forces being higher, but generally we see a linear region from 20% to 70% torque.

To estimate bandwidth of the squeezing mechanism and controller, we commanded a chirp from 1 Hz to 15Hz to the PD motor position loop. Since a total motor displacement between 1,000 and 3,000 degrees was found to be typical across most users, the peak-to-peak amplitude of the chirp was set to a representative 2,000 degrees. We ran the test in both worn and free (i.e. suspended in air) conditions to see how actually wearing the device would impact bandwidth. Both responses versus the commanded input are shown in Fig. 6-a. Aside from higher noise content, the worn condition is generally the same as the free. The -3 dB magnitude cutoff reveals the bandwidth to be approximately 9.7 Hz (Fig 6-b), which, based on our usage thus far, is more than sufficient.

IV. Multisensory VR Interactions

Tasbi's most compelling use is its ability to substitute for interaction forces arising from hand and finger interactions with virtual objects. To demonstrate this, we prototyped a virtual push button (Fig. 10). The onset of interaction is triggered through vibrotactile cues rendered when the user's avatar finger collides with the surface of the button. As the user presses the button inward, proportional squeeze is delivered through the band to convey stiffness. By changing the rate of squeeze, the perceived stiffness can be altered. A second vibrotactile stimulus is rendered when the button is fully depressed. Similar to a "god-object" [24], the avatar hand is projected onto the button surface so that it never appears to penetrate. The illusion of different stiffness levels is also affected by changing the control-display (C/D) ratio between the user's real and avatar hands, such that a stiffer button requires more real-world displacement. Within the haptics community, this visual effect falls under "pseudo-haptics" [25]. Users commented that the combination of vibrotactile, squeeze, and C/D stimuli created a highly intuitive and believable effect.

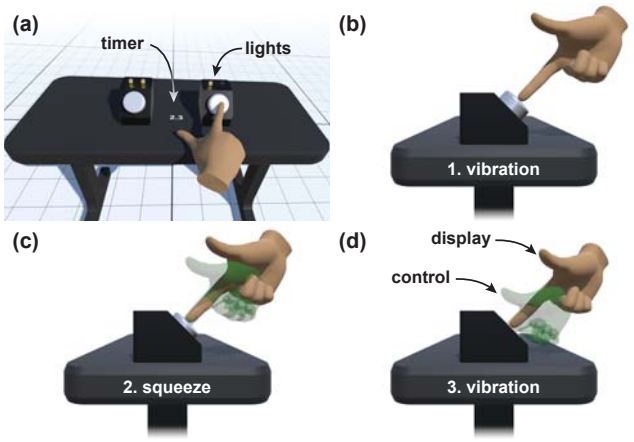

Fig. 10. **(a)** Virtual environment as seen through the HMD. A trial timer was shown along with lights indicating press counts. **(b)** A vibrotactile stimulus is rendered when the finger and button collide. **(c)** Tasbi begins to squeeze proportionally as the button is displaced, with stiffer buttons displaying higher squeeze rates. **(d)** The hidden *control* represents the user's actual position, while the *display* is projected back on to the button surface. Stiffer buttons exhibit a greater discrepancy between the control and display. A second vibrotactile stimulus is rendered when the button bottoms out.

A. Experiment Design

To understand how squeeze haptics and C/D ratios contributed to the button-press, we conducted a method of constants type experiment where users were required to select the "stiffer" of two buttons each trial. Stiffness was parameterized by the combination of K_h, the stiffness depicted through haptic squeeze in units of squeeze per virtual displacement, and K_v, the stiffness depicted through the visual C/D ratio in units of physical displacement per virtual displacement. Thus, higher K_h increased the rate of squeeze as the button was pressed, while higher K_v increased the distance users had to reach their physical hand to achieve a particular button displacement. For both K_h and K_v, seven values were chosen: a Standard value, three Comparison values below the Standard (-Easy, -Medium, -Hard), and three Comparison values above the Standard (+Easy, +Medium, +Hard). Values were determined during a pilot such that users differentiated buttons displaying Easy K_h and K_v values from the Standard with 100% accuracy, Medium values with 75% accuracy, and Hard values slightly above 50% accuracy.

The Standard button *always* displayed Standard K_h and K_v, while the other button was in one of three conditions:

Haptics	A random Comparison K_h and Standard K_v
Visuals	Standard K_h and a random Comparison K_v
Congruent	Congruent Comparison K_h and K_v values

Thus each condition provided both squeeze and C/D stimuli, but in the Haptics condition only squeeze varied the stiffness across trials, while in the Visuals condition only C/D ratio stimuli varied the stiffness. In the Congruent condition *both* squeeze and C/D ratio stimuli varied across trials, matching in difficulty level. Variations of all three conditions were randomly interleaved across 108 trials such that each possible combination was represented six times. The placement of the Standard button was also randomized to either the left or right side. All conditions provided the same vibrotactile stimulus for button contact and bottoming (25 ms, 175 Hz square wave on each tactor). Subjects were given seven seconds and two presses per button to make their decision, which they were encouraged to make as soon as they were confident. A total of 12 subjects participated (6 males, ages 25 to 44, mean 30) in accordance with WIRB #20182617.

B. Results and Discussion

To analyze the results, we assessed the percentage of correct responses overall, the Point of Subjective Equality (PSE), and the Just Noticeable Difference (JND). The accuracy of participant responses was assessed by counting the number of times that they correctly chose the stiffer button for the Easy, Medium, and Hard comparison levels (Fig. 11-a). A two-way ANOVA with repeated measures revealed main effects for both difficulty ($F(2, 22) = 11.7, p < .001$) and condition ($F(1.3, 14.4) = 25.11, p < .001$). Contrasts with a Bonferroni correction showed the Congruent condition produced significantly more accurate responses than the other conditions ($t(11) = 8.7, p < .001$ for Easy, $t(11) = 4.8, p = .001$ for Medium, and $t(11) = 4.7, p = .001$ for Hard). Furthermore, the Congruent condition showed considerably less variance, suggesting more consistent responses overall.

To obtain the JND and PSE values for each condition, we plotted the proportion of correct responses between the Standard and each comparison at the group-level. We then fit this data to three psychometric curves (Fig. 11-bc) using a Generalized Linear Model (GLM) regression. Even though

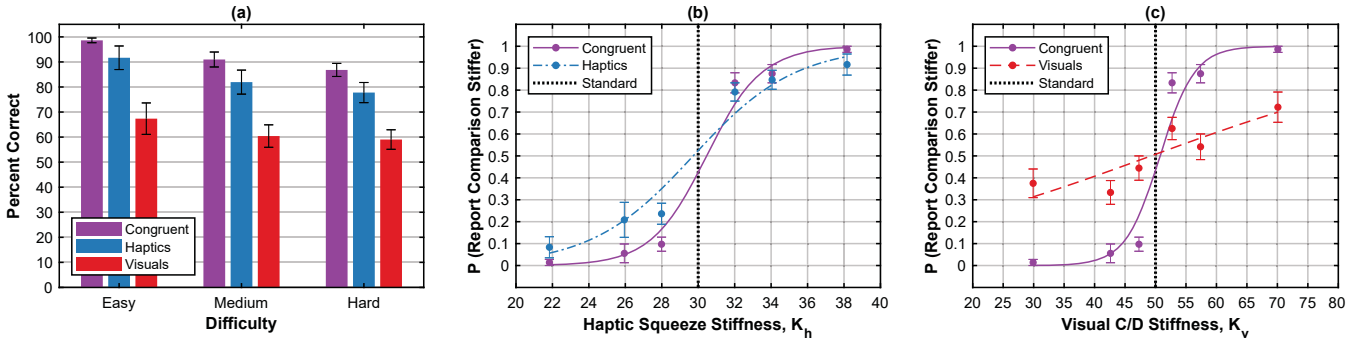

Fig. 11. **(a)** The percent of correctly identified button stiffnesses across all conditions and difficulties. The Congruent condition produced the significantly more accurate responses overall. **(b-c)** Psychometric curves fitted to the group-level data. The Congruent condition displays a higher slope than either of the other conditions. Note that **(b)** and **(c)** have different x-axes. All error bars represent the standard error of the group-level mean.

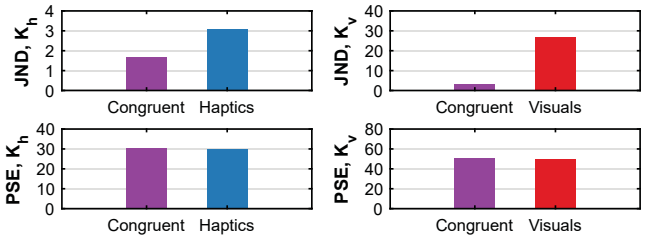

Fig. 12. Just Noticeable Difference (JND) and Point of Subjective Equality (PSE) values obtained from Fig. 11-bc. The Congruent condition displays the smallest JND, and all PSE values correspond with the Standard values.

the visual stiffness K_v was not perfectly titrated to the same difficulty as K_h (despite our efforts in the pilot), there are several interesting observations. First, we can see a steeper curve in the Congruent condition, resulting in a smaller JND than the other two conditions. Fig. 12 shows that the JND decreased by 2-fold for K_h when the C/D ratio also varied, and by 10-fold for K_v when squeeze also varied. The PSE was not affected by the manipulation, and corresponds well with our Standard values. Varying visual and haptic modalities together produces more accurate responses than varying either alone, suggesting that subjects were able to reconcile visual and squeeze based feedback to develop accurate interpretations of virtual stiffness. Overall, our study indicates that wrist based feedback for AR/VR hand interactions is a viable path forward.

V. Conclusions and Future Work

To conclude, we have presented Tasbi, a haptic wristband featuring multisensory squeeze and vibration for AR/VR interactions. The device produces evenly distributed forces up to 15 N and 10 Hz radially around the wrist. Importantly, our design eliminates tangential shear forces which would have otherwise presented problems for band embedded vibrotactors. Finally, we presented a proof of concept application in which squeeze, vibration, and a psuedo-haptic effect were utilized to create a highly believable finger-button interaction.

For future work, the addition of force sensing would enable more consistent squeeze between sessions and individuals, as well as the ability to intelligently respond to disturbances and input forces (e.g. automatically loosening/tightening when a user pulls/pushes the device). Incorporating buttons or a capacitive touch surface would allow for use cases which require bidirectional communication between the user and device. Further miniaturization and integration of batteries and wireless electronics is also of long-term importance, which may necessitate exploration of more exotic actuation methods.

From a psychophysical standpoint, we are most interested in continuing work into sensory substitution. The experiment presented here involving button rendering should be expanded to include varying levels of vibrotactile stimuli as an effect, and other types of force interactions should be explored. Finally, in addition to determining vibrotactor identification rates and squeeze threshold levels, we are interested in researching how squeeze may enhance vibrotactor-skin coupling to ensure consistent stimuli across users.

References

[1] R. Sigrist *et al.*, "Augmented visual, auditory, haptic, and multimodal feedback in motor learning: A review," *Psychonomic Bulletin & Review*, vol. 20, no. 1, pp. 21–53, 2013.

[2] C. Pacchierotti *et al.*, "Wearable haptic systems for the fingertip and the hand: Taxonomy, review, and perspectives," *IEEE Trans. Haptics*, vol. 10, no. 4, pp. 580–600, Oct 2017.

[3] J. Perret and E. Vander Poorten, "Touching virtual reality: a review of haptic gloves," in *ACTUATOR Conf.*, June 2018, pp. 1–5.

[4] H.-Y. Chen *et al.*, "Tactor localization at the wrist," in *EuroHaptics*, 2008, pp. 209–218.

[5] M. Matscheko *et al.*, "Tactor placement in wrist worn wearables," in *Intl. Symp. on Wearable Computers (ISWC)*, Oct 2010, pp. 1–8.

[6] M. G. Carcedo *et al.*, "Hapticolor: Interpolating color information as haptic feedback to assist the colorblind," in *ACM Conf. on Human Factors in Computing Systems (CHI)*. ACM, 2016, pp. 3572–3583.

[7] J. Hong *et al.*, "Evaluating angular accuracy of wrist-based haptic directional guidance for hand movement," in *Graphics Interface Conf.* Canadian Human-Computer Comm. Society, 2016, pp. 195–200.

[8] Y. Zheng and J. B. Morrell, "Haptic actuator design parameters that influence affect and attention," in *IEEE Haptics Symp.*, March 2012, pp. 463–470.

[9] R. Wang *et al.*, "Keep in touch: Channel, expectation and experience," in *ACM Conf. on Human Factors in Computing Systems (CHI)*. New York, NY, USA: ACM, 2012, pp. 139–148.

[10] M. A. Baumann *et al.*, "Emulating human attention-getting practices with wearable haptics," in *IEEE Haptics Symp.*, 2010, pp. 149–156.

[11] D. Tsetserukou, "Haptihug: A novel haptic display for communication of hug over a distance," in *Haptics: Generating and Perceiving Tangible Sensations*, A. M. L. Kappers *et al.*, Eds. Berlin, Heidelberg: Springer Berlin Heidelberg, 2010, pp. 340–347.

[12] A. A. Stanley and K. J. Kuchenbecker, "Evaluation of tactile feedback methods for wrist rotation guidance," *IEEE Trans. Haptics*, vol. 5, no. 3, pp. 240–251, 2012.

[13] S. Casini *et al.*, "Design and realization of the cuff-clenching upper-limb force feedback wearable device for distributed mechano-tactile stimulation of normal and tangential skin forces," in *IEEE Intl. Conf. Intell. Robots and Syst. (IROS)*, 2015, pp. 1186–1193.

[14] S. Song *et al.*, "Hot & tight: Exploring thermo and squeeze cues recognition on wrist wearables," in *Intl. Symp. on Wearable Computers (ISWC)*. New York, NY, USA: ACM, 2015, pp. 39–42.

[15] J. D. Brown *et al.*, "A wrist-squeezing force-feedback system for robotic surgery training," in *IEEE World Haptics Conf.*, June 2017, pp. 107–112.

[16] L. Meli *et al.*, "The hbracelet: A wearable haptic device for the distributed mechanotactile stimulation of the upper limb," *IEEE Robotics and Automation Letters*, vol. 3, no. 3, pp. 2198–2205, July 2018.

[17] F. Chinello *et al.*, "The HapBand: A cutaneous device for remote tactile interaction," in *Haptics: Neuroscience, Devices, Modeling, and Applications*, M. Auvray and C. Duriez, Eds. Berlin, Heidelberg: Springer, 2014, pp. 284–291.

[18] T. K. Moriyama *et al.*, "Development of a wearable haptic device that presents haptics sensation of the finger pad to the forearm," in *IEEE Haptics Symp.*, March 2018, pp. 180–185.

[19] B. Stephens-Fripp *et al.*, "Applying mechanical pressure and skin stretch simultaneously for sensory feedback in prosthetic hands," in *IEEE Intl. Conf. Biomed. Robot. and Biomech.*, 2018, pp. 230–235.

[20] A. Gupta *et al.*, "HapticClench: Investigating squeeze sensations using memory alloys," in *ACM Symp. on User Interface Soft. and Tech. (UIST)*. New York, NY, USA: ACM, 2017, pp. 109–117.

[21] H. Pohl *et al.*, "Squeezeback: Pneumatic compression for notifications," in *ACM Conf. on Human Factors in Computing Systems (CHI)*. New York, NY, USA: ACM, 2017, pp. 5318–5330.

[22] N. Dunkelberger *et al.*, "Conveying language through haptics: A multi-sensory approach," in *Intl. Symp. on Wearable Computers (ISWC)*. Singapore: ACM, Oct 2018.

[23] M. Aggravi *et al.*, "Design and evaluation of a wearable haptic device for skin stretch, pressure, and vibrotactile stimuli," *IEEE Robotics and Automation Letters*, vol. 3, no. 3, pp. 2166–2173, July 2018.

[24] C. B. Zilles and J. K. Salisbury, "A constraint-based god-object method for haptic display," in *IEEE Intl. Conf. Intell. Robots and Syst. (IROS)*, vol. 3, Aug 1995, pp. 146–151 vol.3.

[25] A. Lécuyer, "Simulating haptic feedback using vision: A survey of research and applications of pseudo-haptic feedback," *Presence: Teleoper. Virtual Environ.*, vol. 18, no. 1, pp. 39–53, Jan. 2009.